Fluorescence Correlation Spectroscopy Detects Galanin Receptor Diversity on Insulinoma Cells†

Aladdin Pramanik,*,‡ Magnus Olsson,§ Ülo Langel,§,|| Tamas Bartfai,||,⊥ and Rudolf Rigler‡

Department of Medical Biochemistry and Biophysics, Karolinska Institute, Stockholm, Sweden, and Department of Neurochemistry and Toxicology, Stockholm University, Stockholm, Sweden, Department of PRPN, F. Hoffmann-La Roche Ltd., Basel, Switzerland

Received March 13, 2001; Revised Manuscript Received July 2, 2001

ABSTRACT: Fluorescence correlation spectroscopy (FCS) allows the study of interactions of fluorescently labeled ligand with receptors in living cells at single-molecule detection sensitivity. From the autocorrelation functions of fluorescence intensity fluctuations, the diffusion time of molecules through the confocal volume is analyzed, and from that, the molecular weights of free and bound molecules can be calculated. We have applied FCS to study the receptor diversity for the neuropeptide galanin (GAL) in cultured cells. FCS measurement of the fluorophore rhodamine-labeled GAL (Rh-GAL) has been performed in 0.2-fL confocal volume elements of the laser beam. The analysis of autocorrelation functions of Rh-GAL in solution above cells and at cell membranes demonstrates that the diffusion time of unbound Rh-GAL is 0.16 ms, whereas diffusion times of membrane-bound Rh-GAL are 22 and 700 ms. Because both of the diffusion times (22 and 700 ms) are much longer as compared to that of unbound Rh-GAL, they correspond to slow-diffusing complexes when Rh-GAL is bound to the cell membranes. Addition of excess nonlabeled GAL is accompanied by competitive displacement. Full saturation of the GAL binding is obtained at nanomolar concentrations. Scatchard analysis of binding data reveal one binding process, assuming one binding site per Rh-GAL ($n = 1$). On the other hand, the appearance of two diffusion times, 22 and 700 ms, suggests the existence of two subpopulations of GAL receptor complexes or two subtypes of GAL receptor not detected before. This makes an important point that FCS permits the identification of receptors, which were not possible to detect before by conventional binding techniques. The inhibitory effect of pertussis toxin on the GAL binding considers a G-protein-involved allosteric system, important for the clarification of essential steps in the G-protein-related signal transduction. This study is of pharmaceutical significance, since it will provide insights into how FCS can be used as a rapid technique for studying ligand−receptor interactions in living cells, which is one step forward for large-scale drug screening in cell cultures.

Ligand binding studies on receptors most often require the use of radioactively labeled ligands and include several washing steps to remove unbound ligand. In certain cases, the number of receptors is few per cell, and no specific binding is detected because of high background. In addition, the half-life of the receptor−ligand complex is often shorter or similar to the time required for separations of unbound and bound ligand, respectively. Interactions between certain ligands and their different receptor subtypes are, therefore, often overlooked by the conventional equilibrium binding technique.

Fluorescence correlation spectroscopy (FCS)[1] is a powerful biophysical tool for examining molecular interactions with very high specificity. In this technique, the fluorescence of single dye-labeled molecules excited by a sharply focused laser beam is observed. From the fluorescence intensity fluctuations, due to variations in the number of molecules in the laser volume element of observation, the average number of molecules can be directly obtained using the intensity correlation function. Furthermore, from the characteristic correlation times, dynamic processes such as Brownian motion can be analyzed. This technique was introduced in the early 1970s (*1*−*3*), but only recently it has become applicable to bioscience because of a substantial increase in sensitivity (*4*), allowing single-molecule analysis (*5*, *6*). The tiny laser volume elements (0.2 fL) in which the measurements are performed make it possible to evaluate molecular processes at the cell membrane (*7*−*14*). This technique permits the identification of receptors or target

† This work was supported by the Swedish National Academy of Sciences.

* Corresponding author telephone: +46 8 728 68 07; fax: +46 8 32 65 05; e-mail: aladdin.pramanik@mbb.ki.se.

‡ Karolinska Institute.

§ Stockholm University.

|| Present address: The Harold L. Dorris Neurological Research Center, Department of Neuropharmacology, The Scripps Research Institute, La Jolla, CA

⊥ Hoffmann-LaRoche Ltd.

[1] Abbreviations: FCS, fluorescence correlation spectroscopy; GAL, galanin; GALR2, GAL receptor subtype 2; GALR1, GAL receptor subtype 1; Rh, rhodamine (tetramethylrhodamine-5-(and-6)-isothiocyanate); Rh-GAL, rhodamine-labeled GAL; HPLC, high-performance liquid chromatography.

10.1021/bi010514q CCC: $20.00
Published on Web 08/15/2001

molecules that was not possible to detect before by isotope labeling. With FCS, one can analyze a mixture of multiple components possessing different molecular weights and different diffusion times, respectively. The beauty of the FCS technique is that there is no need for separating unbound from bound ligand (*7*) to calculate the receptor-bound and free-ligand fractions. Moreover, molecular interactions can be analyzed rapidly (2−5 s) in small volumes (1−5 μL). It must be mentioned that with conventional binding methods one attempts to concentrate the samples, while with FCS one can analyze very diluted samples. Thus, it is possible to perform large-scale drug screening both in solutions and in cell cultures using the FCS technique.

The appearance of Alzheimer amyloid β-peptide aggregates in solution (*15*) and cerebrospinal fluid of Alzheimer's patients (*16*) has been reported using FCS, and FCS is suggested as a diagnostic tool. FCS has been applied to study precisely ligand−receptor interactions for the purified acetylcholine (*17*) and serotonin (*18*, *19*) receptors in solution. Using FCS, we have been able to discover a receptor for the C-peptide of proinsulin (*8*, *20*) and for the neuroactive kavain (*9*) in cultured cells. Recently, we have been able to demonstrate the C-peptide specific binding to macromolecules obtained from detergent-solubilized cell materials by using FCS, which was not possible to detect before (*11*), confirming our discovery that C-peptide binds specifically to membranes of intact living cells (*8*). Very recently, the interaction of the protein p53 with DNA has been studied using FCS, allowing an understanding of the mechanism for the p53 latency (*21*). FCS also allows the study of apoptosis because it has been possible to estimate hydrogen peroxide concentrations (which causes apoptosis) in apoptotic cells in vivo using FCS, demonstrating how hydrogen peroxide, produced in apoptotic cells, spreads out and kills neighboring healthy cells (*22*).

Galanin (GAL) is a neuroendocrine peptide that displays a variety of important biological actions and is thought to be implicated in several human disorders such as Alzheimer's disease, depression, and feeding disorders (for references, see a review in ref *23*). We have now applied FCS to study the existence of different subpopulations or subtypes of GAL receptors in cultured pancreatic insulinoma cells (Rinm5F). Rinm5F cells have been shown to possess the GAL receptor subtype 2 (GALR2) (*24*). Both Rinm5F and Rin14B cell lines are derived from the pancreas. Because Rinm5F and Rin14B lines are closely related to each other and Rin14B cell lines have been shown to express the GAL receptor subtype 1 (GALR1) in high levels (*25*), it is possible that the Rinm5F cell lines can also express GALR1. Therefore, it was of interest to study GAL receptor diversity in Rinm5F cell lines. To provide a fluorescence signal, GAL has been labeled by the fluorophore rhodamine (Rh). Evidence is presented that GAL is bound to different subpopulations or subtypes of membrane-bound GAL receptors.

MATERIALS AND METHODS

Materials. The fluorophore rhodamine (tetramethylrhodamine-5-(and-6)-isothiocyanate) was purchased from Molecular Probes (Leiden, The Netherlands). Pertussis toxin and all other reagents were from Sigma Chemical Co., St. Louis, MO.

Labeling of GAL. The synthesis and purification of GAL have been described earlier in detail (*26*). Porcine GAL was labeled with rhodamine at 5−10-fold molar excess of the reagent. One milligram (0.31 mmol) of porcine GAL was dissolved in 0.1 M $NaHCO_3$, pH 8.9. A total of 0.6 mg (1.3 mmol) of tetramethylrhodamine isothiocyanate (Rh) was dissolved in dimethylformaldehyde. The Rh solution was slowly added to the GAL solution during intense stirring, and the reaction mixture was incubated for 1 h at room temperature. After 1 h, the reaction was terminated. The products were purified by HPLC on a reversed-phase C_{18} column. Four different peptide peaks were eluted, three of which were Rh-labeled products, and one was unreacted GAL. The products were analyzed with mass spectrometry, which revealed that one product was a biRh-GAL (double-rhodamine-labeled GAL), and the two other peaks corresponded to single-labeled GAL derivatives. There are basically two possible incorporation sites for Rh to GAL: the N terminus of the peptide and the ϵ-amino group of Lys^{25} in the GAL sequence. The double-labeled product was probably due to incorporation of Rh in both of those positions, and the two other labeled products were the single incorporations of Rh to Lys^{25} and the N terminus, respectively. In our experiment, the Lys^{25}-Rh-GAL was used as a fluorescence probe.

Cell Culture. Insulinoma cells were grown to 50% confluency in Gibco RPMI 1640 medium with L-glutamine supplemented with fetal calf serum (5%, v/v), penicillin (50 U/mL), and streptomycin (50 U/mL) in an atmosphere of 5% (v/v) CO_2-enriched air at 37 °C.

FCS Instrumentation. FCS was performed with confocal illumination of a laser volume element of 0.2 fL in a ConfoCor instrument (Carl Zeiss-Evotec, Jena, Germany; Figure 1) as described previously (*4*). As focusing optics, a Zeiss Neofluar 40 × NA 1.2 objective for water immersion was used in a epi-illumination setup. To separate excited from emitted radiation, a dichroic filter (Omega 540 DRL PO_2) and a band-pass filter (Omega 565 DR 50) were used. The Rh-GAL was excited with the 514.5-nm line of an argon laser. The intensity fluctuations were detected by an avalanche photodiode (EG and SPCM 200) and were correlated with a digital correlator (ALV 5000, ALV, Langen, Germany). Measurements were performed in solution and on cells cultured in Nunc chambers (Nalge Nunc Inc., IL) with Rh-GAL added. With the objective used (40 × NA 1.2), a 0.2-fL volume element was illuminated with dimensions of $\omega = 0.25$ μm and $z = 1.25$ μm. To avoid photobleaching, the exciting intensity was adjusted such that the detected photon count rate did not exceed 4000−5000 counts per molecule per second (*27*).

FCS Binding Experiment. All binding studies with FCS were carried out on cells cultured in eight-well Nunc chambers at 20 °C. Prior to the experiments, cells were washed 5× with PBS (NaCl, 137 mM; KCl, 2.7 mM; KH_2PO_4, 1.5 mM; $Na_2HPO_4 \cdot 2H_2O$, 8.1 mM; pH 7.4) and incubated with binding buffer (Hepes, 20 mM; NaCl, 140 mM; KCl, 5 mM; $MgCl_2$, 1.2 mM; Na_2CO_3, 3.3 mM; glucose, 5.5 mM; $CaCl_2$, 1.8 mM; pH 7.4) containing Rh-

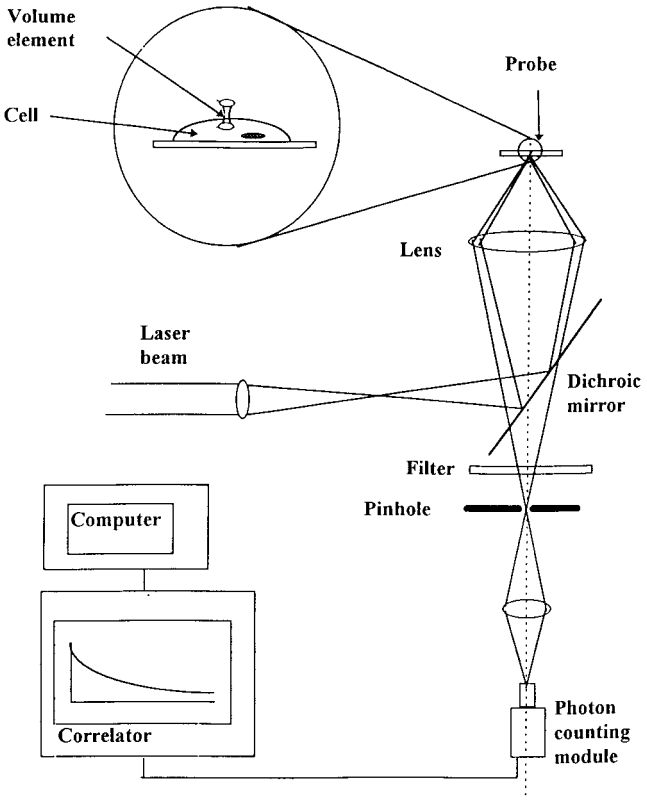

FIGURE 1: FCS setup. The laser beam from an argon ion laser is sharply focused via a dichroic mirror and a lens to form a tiny confocal volume element (0.2 fL). The laser beam is projected from below into an eight-well Nunc chamber containing a monolayer of cultured cells and rhodamine-labeled ligand (see magnified diagram). After excitation of the labeled ligand, emitted light is transmitted via the dichroic mirror, a band-pass filter, and a pinhole to a photodetector. The volume element is positioned onto the cell surface for detection of ligand binding. The dimensions of the laser beam focus and the pinhole together define the confocal volume element. The detector signal is fed into a digital signal correlator, which computes online in real time the autocorrelation function of the detected intensity fluctuations.

GAL at room temperature. Binding of GAL was measured after 60 min of incubation of cells in the presence of 5 nM Rh-GAL. Experiments for binding isotherm were performed after 60 min of incubation of cells with different concentrations of Rh-GAL. Specificity of the Rh-GAL binding was demonstrated by the competitive displacement of bound Rh-GAL from cell surfaces after 3 h of incubation of 5 μM nonlabeled GAL added to cells (postincubation). Specific binding was also demonstrated by the inability of the Rh-GAL to bind to cell surfaces when cells were preincubated with nonlabeled GAL for 1−3 h. In a similar fashion, competetive displacement was evaluated after pre- and postincubations with M40, a GAL antagonist. Cells were pretreated with pertussis toxin (1 μg/mL) at 37 °C for 4 h under 95% O_2 and 5% CO_2 before binding studies were carried out.

FCS Data Evaluation. (*a*) *Brownian Motion of Rh-GAL and Analysis of Ligand−Receptor Binding on the Cell Surface.* Fluorescence intensity fluctuations occuring in a volume element are correlated (*1*−*3*), and nonlinear least-squares minimization (*28*) is used to calculate the parameters of the intensity autocorrelation function $G(\tau)$. $G(\tau)$ for 3D diffusion of the unbound Rh-GAL in solution and 2D diffusion of the bound Rh-GAL to membranes on the cell surface is given by

$$G(\tau) = 1 + \frac{1}{N}\left[(1 - \sum y_i)\left(\frac{1}{1 + \frac{\tau}{\tau_D^F}}\right)\left(\frac{1}{1 + \left(\frac{\omega}{z}\right)^2 \frac{\tau}{\tau_D^F}}\right)^{1/2} + \sum y_i \left(\frac{1}{1 + \frac{\tau}{\tau_D^{B_i}}}\right)\right] \quad (1)$$

where diffusion time τ and diffusion coefficient D are related as $\tau = w^2/4D$, y_i is the fraction of membrane-bound Rh-GAL diffusing with diffusion time $\tau_D^{B_i}$, and $(1 - \sum y_i)$ is the fraction of unbound Rh-GAL diffusion with diffusion time τ_D^F. The relative fraction of cell-surface-bound GAL ligand ($\sum y_i$) is obtained at an increasing concentration of Rh-GAL. The Scatchard representation of the mass action law is obtained from

$$\frac{\sum y_i}{(1 - \sum y_i)R_o} = \sum K_i \left(n_i - \frac{y_i L_o}{R_o}\right) \quad (2)$$

where K_i and n_i are the association constant and the number of ligand binding sites per receptor molecule, respectively. L_o is the total ligand concentration. R_o, the total receptor concentration, cannot be determined independently but was calculated from the maximum number of bound ligand molecules at saturation, assuming one binding site for one receptor molecule ($n = 1$).

(*b*) *Distribution of Diffusion Time of Ligand−Receptor Complexes with CONTIN Algorithm.* Instead of evaluating discrete diffusion processes with distinct species (y_i) and their characteristic diffusion times (τ_{D_i}), the dynamic motion of receptor complexes in membranes can be distributed with regard to their diffusion times using a distribution function $P(\tau_{D_i})$. To assess the validity of the presence of discrete ligand−receptor complexes, we analyzed $G(\tau)$, representing the distribution of diffusion times according to an expression of multiple components:

$$G(\tau) = 1 + \frac{1}{N}\int_i P(\tau_{D_i}) \frac{1}{1 + \frac{\tau}{\tau_{D_i}}}\left(\frac{1}{1 + \left(\frac{\omega}{z}\right)^2 \frac{\tau}{\tau_{D_i}}}\right)^{1/2} d\tau_{D_i} \quad (3)$$

where $P(\tau_{D_i}) = \sum y_i \, dy$, representing the distribution of diffusion time τ_{D_i}. This represents a model-independent analysis of the diffusion processes observed by the correlation function. For evaluation of the distribution function, the CONTIN algorithm was applied (*29*, *30*).

RESULTS

Binding of Rhodamine-Labeled GAL (Rh-GAL) to the Cell Surface. Intensity autocorrelation functions $G(\tau)$ of Rh-GAL in solution and bound to cell membranes are presented in Figure 2, panels A and B, respectively. Analysis of $G(\tau)$ demonstrates that the diffusion time (τ_{D_1}) of unbound Rh-GAL is 0.16 ms (Figure 2A). As shown in Figure 2B, there are two diffusion times, $\tau_{D_2} = 22$ ms and $\tau_{D_3} = 700$ ms. Both the τ_{D_2} and the τ_{D_3} are much longer as compared to the τ_{D_1}. The total binding of Rh-GAL to cell membranes is in the range of 65−75%.

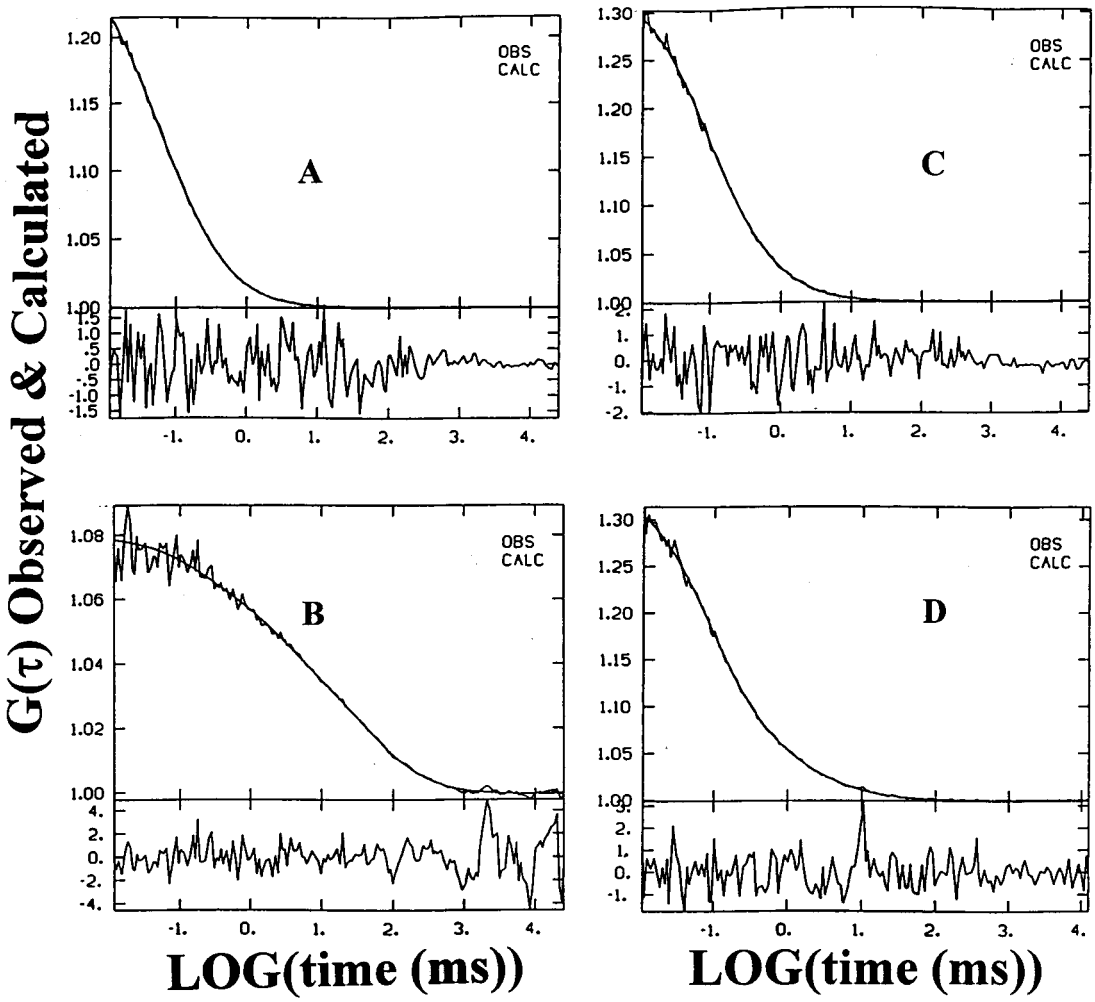

FIGURE 2: GAL binding and displacement to the membranes of cultured insulinoma cells. Autocorrelation functions $G(\tau)$ of Rh-GAL (5 nM) free in solution (A) and bound to membranes on the cell surfaces (B). Diffusion times (τ_D) and corresponding fractions (y): $\tau_{D_1} = 0.16$ ms, $y_1 = 35\%$ (A); $\tau_{D_2} = 22$ ms, $y_2 = 53\%$ and $\tau_{D_3} = 700$ ms, $y_3 = 12\%$ (B). y_1 is an unbound fraction; y_2 and y_3 are bound fractions. Total binding is calculated in a percentage as follows: total binding $= y_2 + y_3/y_1 + y_2 + y_3$. $G(\tau)$ of displacement of cell membrane-bound Rh-GAL by a 1000-fold molar excess of nonlabeled GAL (C) and nonlabeled M40 (D) after postincubations. In postincubations, insulinoma cells were first incubated with binding buffer containing 5 nM Rh-GAL for 60 min, and observed binding was treated as the control. Then, 5 μM nonlabeled GAL or nonlabeled M40 was added to the same cells, incubated for 3 more h, and checked for displacement. In preincubations, cells were first incubated with binding buffer containing 5 μM nonlabeled GAL or nonlabeled M40 for 60 min, and then, 5 nM Rh-GAL was added to the same cells and checked for binding during another 3 h.

Saturation of Binding. To test whether the Rh-GAL binding to specific receptors in cell membranes is concentration dependent and saturable, we carried out binding experiments at different concentrations of Rh-GAL. As seen in Figure 3, the increasing concentrations of Rh-GAL clearly lead to the elevation of binding, and the binding is saturated at nanomolar concentrations. From the Scatchard plot (Figure 3, insert; eq 2) of the binding isotherm, we obtain the binding constant $K_{assoc} = 0.8 \times 10^9$ M^{-1} and $n = 1$.

Specificity and Kinetics of Binding. To check that the Rh-GAL binding to the cell membranes is not only ligand concentration dependent and saturable but also specifically displaced by nonlabeled GAL, we studied Rh-GAL binding in the presence of a 1000-fold molar excess of nonlabeled GAL. We incubated the cells with Rh-GAL, and after 60 min of incubation, we measured binding, treated as control, and then we added nonlabeled GAL to cells and observed binding with time course. As shown in Figure 4, with time course, the presence of nonlabeled GAL in cells resulted in a drop of Rh-GAL binding, and about 75% of total binding was specifically displaced after 3 h of incubation with nonlabeled GAL (5 μM). The autocorrelation function of this displacement and its CONTIN distribution are presented in Figures 2C and 5C, respectively. Similar displacement was observed when Rh-GAL binding was studied in the presence of a 1000-fold molar excess of nonlabeled M40, a GAL antagonist (Figure 2D). Moreover, the Rh-GAL was unable to bind to cell membranes within 1−3 h when cells were first preincubated with nonlabeled GAL for 1 h, and then, Rh-GAL was added to the cells, indicating that GAL receptors are already occupied with nonlabeled GAL. In this case, only the nonspecific binding is observed (data not shown). Plotting of the dissociation curve in log scale of the y-axis (binding) and lineal scale of the x-axis (time) (Figure 4, insert) showed a straight line, indicating that displacement occurred in monoexponential mode. Furthermore, analysis of the dissociation curve yields a dissociation time (τ_{dissoc}) of 2700 s and a dissociation rate constant (k_{dissoc}) calculated as $k_{dissoc} = 1/\tau_{dissoc} = 3.7 \times 10^{-4}$ s^{-1}. From knowledge of the dissociation time and the K_{assoc} ($K_{assoc} =$

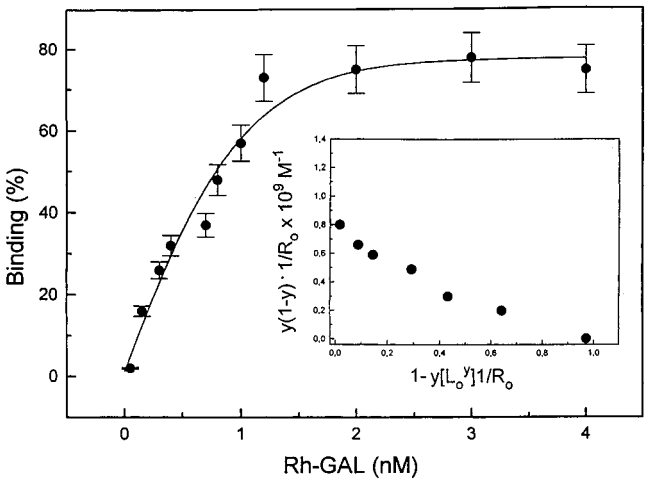

FIGURE 3: GAL binding curve. Binding of Rh-GAL to cell membranes of insulinoma cells. Fractional saturation of the membrane-bound Rh-GAL (y) as a function of the ligand concentration (L_o) in the binding medium. Cells were incubated with binding buffer containing different concentrations of Rh-GAL for 60 min. Scatchard plot is shown as an insert. Each data point represents the mean of at least six separate measurements. "y" = bound ligand, "$1 - y$" = free ligand, R_o = total receptor concentration, and L_o = total ligand concentration.

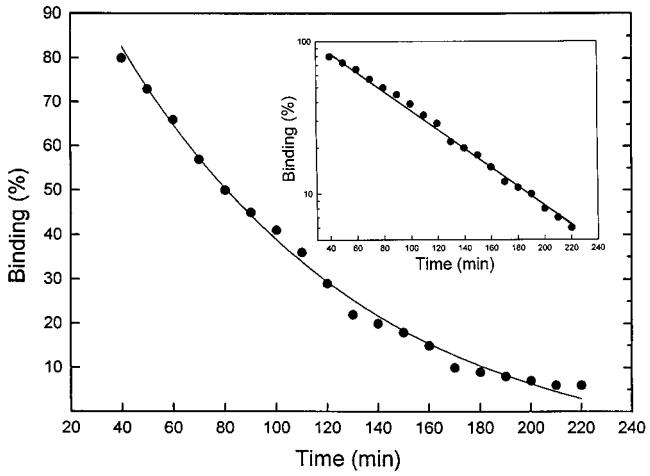

FIGURE 4: Time course of displacement of Rh-GAL binding by nonlabeled GAL. Cells were incubated with binding buffer containing 5 nM Rh-GAL for 60 min. Then 5 μM nonlabeled GAL was added to the cells, and FCS measurements were carried out at time intervals as shown in the x-axis. Each data point represents the mean of at least six separate measurements. Log scale for the displacement of the binding process is shown as an insert.

0.8×10^9 M^{-1}; see above), the association rate constant (k_{assoc}) can be obtained as follows:

$$k_{assoc} = K_{assoc} k_{dissoc} = 3 \times 10^5\ M^{-1}\ s^{-1}$$

Presentation of Ligand−Receptor Complexes with Distribution of Diffusion Times. A model-independent analysis of the diffusion processes (eq 3) as has been applied previously for presenting ligand−receptor complexes (*8*) is presented in Figure 5. There are three peaks that show distributions of diffusion times of τ_{D_i} corresponding to unbound Rh-GAL and to receptor-bound Rh-GAL, that is, these three peaks represent three different species of Rh-GAL: one free (τ_{D_1}) and two bound (τ_{D_2} and τ_{D_3}). Distributions of $\tau_{D_1} = 0.16$ ms (Figure 5A) correspond to unbound Rh-GAL (Figure 2A). Distributions of $\tau_{D_2} = 22$ ms and $\tau_{D_3} = 700$ ms (Figure 5B) correspond to receptor-bound Rh-GAL (Figure 2B). As expected, in the presence of a 1000-fold molar excess of nonlabeled GAL, the two peaks ($\tau_{D_2} =$ 22 ms and $\tau_{D_3} = 700$ ms) corresponding to ligand−receptor complexes disappeared due to competitive displacement by nonlabeled GAL (Figure 5C).

Effect of Pertussis Toxin on the Ligand Binding. It has been earlier shown in vitro that GAL receptor belongs to a G-protein coupled receptor family (*31*). To test whether the GAL binding in living cells is also accompanied by G-protein involvement, we pretreated cells with pertussis toxin. As shown in Figure 5D, this resulted in complete loss of the slowly diffusing GAL receptor component, leaving a small component of rapidly diffusing (1−3 ms) complexes (~15%) that could not be further displaced by addition of excess of unlabeled GAL. However, when pertussis toxin pretreated cells were exposed to Rh-GAL concentrations of 50−100 nM, the rapidly diffusing GAL binding complex increased to 45−50%, and this component could be displaced very rapidly (within 10 min) by addition of unlabeled GAL.

DISCUSSION

In FCS measurements, the fluorescence intensity fluctuations are recorded from only those molecules that diffuse through the confocal laser volume element. The time required for the passage of fluorescent molecules through the volume element is determined by the diffusion coefficient, which is related to the size of a molecule. Thus, diffusion times obtained from the analysis of fluorescence intensity fluctuations with autocorrelation functions allow one to differentiate faster diffusing and slower diffusing molecules as an analogy for unbound and bound states of ligand molecules, i.e., presentation of free ligand and ligand−receptor complexes. This analogy is generally valid for a molecular size in solution. It is also valid for a molecular size at the cell membrane under certain conditions. However, in living cells, under certain conditions, one should not exclude that the difference in the viscosity between the aqueous environment and the plasma membrane may provide a basis for the analogy of unbound to bound ligand. Because the diffusion times of 22 and 700 ms (Figures 2B and 5B) are much longer as compared to 0.16 ms of unbound Rh-GAL (Figures 2A and 5A), they correspond to complexes where Rh-GAL is bound to GAL receptors.

Full saturation of Rh-GAL binding at nanomolar concentration (Figure 3) provides evidence for a strong affinity binding site. Both the shape of the Scatchard plot and its n value ($n = 1$) suggest one receptor binding site per GAL. The 75% displacement of the Rh-GAL binding to cell membranes by an excess of nonlabeled GAL confirms that binding is specific for GAL receptors. Moreover, the specificity of binding was also verified by the fact that Rh-GAL was unable to bind to cell membranes within 1−3 h, when GAL receptors are already occupied with nonlabeled GAL by 1 h of preincubation of cells with excess nonlabeled GAL. The dissociation rate constant of 3.7×10^{-4} s^{-1} allows one to conclude that the Rh-GAL binding is long lasting and that GAL binds to receptors with strong affinity. Displacement of the Rh-GAL binding by excess nonlabeled M40, a GAL antagonist (Figure 2D), reconfirms the specific-

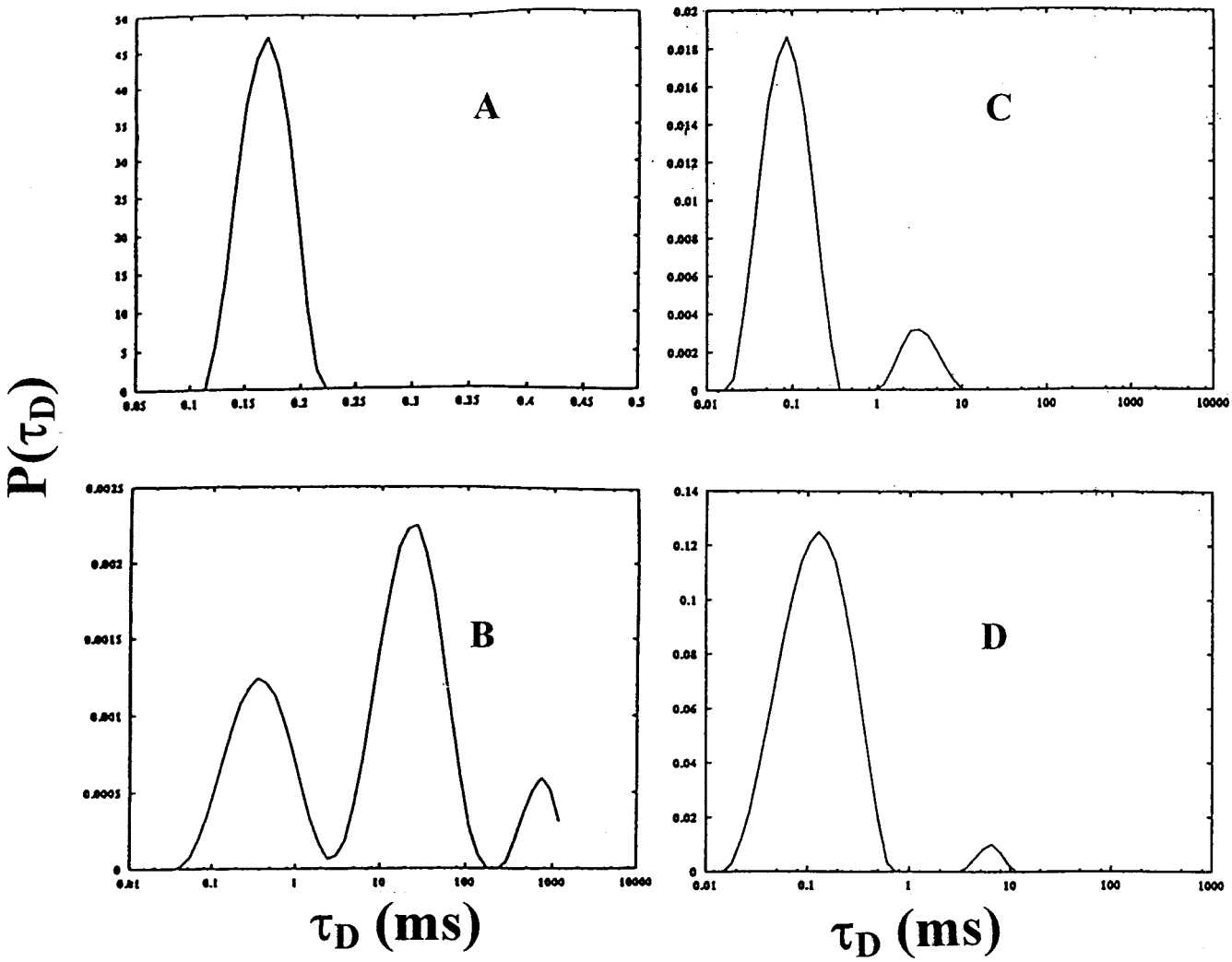

FIGURE 5: CONTIN distributions of diffusion times $P(\tau_{D_i})$ of GAL binding and displacement to the membranes of cultured insulinoma cells. Rh-GAL free in solution (A), binding of Rh-GAL to the cell membranes (B), displacement of membrane-bound Rh-GAL by postincubation of a 1000-fold molar excess of nonlabeled GAL (C), and inhibition of membrane-bound Rh-GAL by pertussis toxin (D).

ity of the binding. Because M40 antagonizes GAL binding from its receptors, this clearly shows that binding observed on the cell membrane occurs via GAL binding sites on a receptor.

As compared to conventional binding methods, with FCS, one can analyze the affinity and specificity of a ligand and subpopulations or subtypes of receptors directly, not including any separation steps. The next important point is that, since in FCS technique diffusion times of a ligand molecule and ligand−receptor complexes are used as characteristic parameters for binding analysis, distribution of diffusion times presents a clear-cut appearance of binding complexes (*8*). Thus, the appearance of two binding complexes (Figure 5B) through distribution of diffusion times suggests that these are representations of two different subpopulations of GAL receptor complexes or subtypes of GAL receptors. Because the GAL binding is competitively displaced, these two diffusion times represent two different specific interaction sites on the plasma membrane. Again, this could be explained either by two different subtypes of GAL receptor or by one receptor type but in different sets of protein complexes. Finally, the appearance of two different ligand−receptor complexes clearly suggests that Rh-GAL does not bind to a single homogeneous population but to a heterogeneous population of receptors, which could be either two subpopulations or subtypes of receptors. However, we do not preclude that some of the GAL receptors may bind to other proteins or to each other in a higher oligomeric state, thus moving with differential speed. It is less likely that a heterogeneously glycosylation of the extracellular part of the receptor or the internalization of the GAL receptor upon Rh-GAL binding may relate to two different diffusion times observed by FCS.

This finding makes an important point that FCS permits the identification of receptors or subpopulations of receptor complexes that was not possible to detect before by other conventional binding techniques, convincing one that a FCS ligand−receptor interaction can be analyzed quantitatively on the cell membrane with a sensitivity and spatial resolution unparalleled so far. Moreover, the discovery of new GAL subtype receptors or subpopulations of receptors may be an answer to the question of why the neuropeptide GAL displays multiple functions.

The fact that exposure of the cells to pertussis toxin interferes with the GAL binding to its receptors (Figure 5D) provides evidence for the involvement of G-proteins in the signal-transduction pathway in living cells. With detailed structural (*32*) and functional (*33*) data on G-proteins accumulating, the hypothesis may be considered that a

G-protein, which interacts with a ligand-activated receptor, could constitute an allosteric system involving at least two or possibly several conformational states of both the receptor and the G-protein. Following interaction with the specific ligand, certain conformations may become stabilized, which may affect the interaction with the G-protein.

Pertussis toxin is known to affect a cysteine residue in the C-terminal chain of the α-subunit of the G-protein, which interacts with loop regions of the membrane-spanning receptor, thus interfering with the interaction between the G-protein and the receptor (*32*). Preincubation of cells with pertussis toxin in the present study was found to abolish the binding of GAL to the membrane. This finding may be explained as the result of allosteric actions according to the principle of detailed balance, involving at least two or possibly several conformational states of both the receptor and the G-protein (*34*). Addition of Rh-GAL at 50 nM and higher concentrations to cells pretreated with pertussis toxin reveals a rapidly diffusing GAL receptor complex ($\tau_D = 1-3$ ms), which, in part, can be displaced within a few minutes with an excess (5 μM) of unlabeled GAL (data not shown). These observations are compatible with the existence of at least two different GAL receptor complexes corresponding to two subtypes of GAL receptors or subpopulations of GAL receptors, one with low affinity and high mobility and another with high affinity and low mobility. Thus, 22-ms species correspond to a receptor with low affinity but high mobility, and 700-ms species correspond to a receptor with high affinity but low mobility. One of the possible explanations of the inhibitory effects of pertussis toxin on both the 22-ms and the 700-ms species is that GAL would preferably bind the high-affinity receptor conformation (700-ms species), i.e., the receptor in complex with the G−α,*β*,*γ*−GDP (G-protein−α,*β*,*γ*-subunits−GDP) as well as even bind to the low-affinity receptor state (22-ms species) when G-protein is partly released from receptors. Our results contribute new insight into the molecular mechanism of the signal-transduction pathway based on studies in living cells by a new type of molecular spectroscopy (FCS) and are important for the clarification of essential steps in the G-protein-related signal transduction.

ACKNOWLEDGMENT

We gratefully acknowledge the excellent technical assistance of Ms. Ebba Hagman and Ms. Brith Larsson.

REFERENCES

1. Magde, D., Elson, E. L., and Webb, W. W. (1972) *Phys. Rev. Lett. 29*, 705−711.
2. Elson, E. L., and Magde, D. (1974) *Biopolymers 13*, 1−27.
3. Ehrenberg, M., and Rigler, R. (1974) *Chem. Phys. 4*, 390−401.
4. Rigler, R., Mets, Ü., Widengren, J., and Kask, P. (1993) *Eur. Biophys. J. 22*, 169−175.
5. Rigler, R., and Mets, Ü. (1992) *SPIE Laser Spectrosc. Biomol. 1921*, 239−248.
6. Eigen, M., and Rigler, R. (1994) *Proc. Natl. Acad. Sci. U.S.A. 91*, 5740−5747.
7. Rigler, R. (1995) *J. Biotechnol. 41*, 177−186.
8. Rigler, R., Pramanik, A., Jonasson, P., Kratz, G., Jansson, O. T., Nygren, P.-Å., Ståhl, S., Ekberg, K., Johansson, B.-L., Uhlén, S., Uhlén, M., Jörnvall, H., and Wahren, J. (1999) *Proc. Natl. Acad. Sci. U.S.A. 96*, 13318−13323.
9. Boonen, G., Pramanik, A., Rigler, R., and Häberlein, H. (2000) *Planta Med. 66*, 7−10.
10. Pramanik, A., and Rigler, R. (2000) in *Fluorescence Correlation Spectroscopy*: *Theory and Applications* (Elson, E. L., and Rigler, R., Eds.) pp 101−131, Springer-Verlag, Berlin.
11. Henriksson, M., Pramanik, A., Shabqat, J., Zhong, Z., Tally, M., Ekberg, K., Wahren, J., Rigler, R., Johansson, J., and Jörnvall, H. (2001) *Biochem. Biophys. Res. Commun. 280*, 423−427.
12. Pramanik, A., and Rigler, R. (2001) *Biol. Chem. 382*, 371−378.
13. Pramanik, A., Ekberg, K., Zhong, Z., Shabqat, J., Henriksson, M., Tibell, A., Tally, M., Wahren, J., Jörnvall, H., Rigler, R., and Johansson, J. (2001) *Biochem. Biophys. Res. Commun. 284*, 94−98.
14. Zhong, Z., Pramanik, A., Ekberg, K., Jansson, O. T., Wahren, J., and Rigler, R. *Diabetologia*, in press.
15. Tjernberg, L., Pramanik, A., Björling, S., Thyberg, P., Thyberg, J., Nordstedt, C., Terenius, L., and Rigler, R. (1999) *Chem. Biol. 6*, 53−62.
16. Pitschke, M., Prior, R., Haupt, M., and Riesner, D. (1998) *Nat. Med.* (*NY*) *4*, 832−834.
17. Rauer, B., Neumann, E., Widengren, J., and Rigler, R. (1996) *Biophys. Chem. 58*, 3−12.
18. Tairi, A.-P., Hovius, R., Pick, H., Blasey, H., Bernard, A., Suprenant, A., Lundström, K., and Vogel, H. (1998) *Biochemistry 37*, 15850−15864.
19. Wohland, T., Friedrich, K., Hovius, R., and Vogel, H. (1999) *Biochemistry 38*, 8671−8681.
20. Wahren, J., Ekberg, K., Johansson, J., Henriksson, M., Pramanik, A., Johansson, B.-L., Rigler, R., and Jörnvall, H. (2000) *Am. J. Physiol. 278*, E759−E768.
21. Yakovleva, T., Pramanik, A., Kawasaki, T., Tan-no, K., Gileva, I., Reznokov, K., Lindegren, H., Langel, Ü., Ekström, T. J., Rigler, R., Terenius, L., and Bakalkin, G. *J. Biol. Chem.*, in press.
22. Reznikov, K., Kolesnikova, L., Pramanik, A., Tan-no, K., Gileva, I., Yakovleva, T., Rigler, R., Terenius, L., and Bakalkin, G. (2000) *FASEB J. 14*, 1754−1764.
23. Bartfai, T., Hökfelt, T., and Langel, Ü. (1993) *Crit. Rev. Neurobiol. 7*, 229−274.
24. Howard, A., Tan, C., Shiao, L.-L., Palyha, O., McKee, K., Weinberg, D., Feighner, S., Cascieri, M., Smith, R., Van Der Ploeg, L., and Sullivan, K. (1997) *FEBS Lett. 405*, 285−290.
25. Parker, E., Izzarelli, D., Nowak, H., Mahle, C., Iben, L., Wang, J., and Goldstein, E. (1995) *Mol. Brain Res. 34*, 179−189.
26. Land, T., Langel, Ü., Fisone, G., Bedecs, K., and Bartfai, T. (1991) *Methods Neurosci. 5*, 225−234.
27. Wennmalm, S., and Rigler, R. (1999) *J. Phys. Chem. B 103*, 2516−2519.
28. Marquardt, D. W. (1963) *J. Soc. Ind. Appl. Math. 11*, 431−441.
29. Provencher, S. W. (1982) *Comput. Phys. Commun. 27*, 213−227.
30. Provencher, S. W. (1982) *Comput. Phys. Commun. 27*, 229−242.
31. Fisone G., Langel, U., Carlquist, M., Bergman, T., Consolo, S., Hokfelt, T., Unden, A., Andell, S. and Bartfai, T. (1989) *Eur. J. Biochem. 181*, 269−276.
32. Hamm, H. E. (1999) *J. Biol. Chem. 279*, 669−672.
33. Farfel, Z., Bourne, H. R., and Iiri, T. (1999) *N. Engl. J. Med. 340*, 1012−1020.
34. Monod, J., Wyman, J., and Changeux, J. P. (1965) *J. Mol. Biol. 12*, 88−118.

BI010514Q